Coupling Matrix Extraction and Reconfiguration Using a Generalized Isospectral Flow Method

Stefan Pflüger, Christian Waldschmidt, *Senior Member, IEEE*, and Volker Ziegler, *Senior Member, IEEE*

***Abstract*—The coupling matrix model is a helpful tool during synthesis and analysis of coupled resonator filters. Application of the coupling matrix for filter synthesis often requires the designer to reconfigure the coupling matrix to yield a specific matrix structure matching the topology of the filter. Currently, there is no closed-form solution known to this matrix reconfiguration problem. This paper proposes a new approach to solve this problem for coupling matrix representations of general lossy filters. The method is based on infinitesimal matrix rotations and can be considered as a continuous analog to the well-known coupling matrix similarity transforms. The results shown indicate good convergence behavior of the reconfiguration algorithm, as well as the ability of the method to always keep the desired scattering parameter goal. Based on this algorithm, a method for coupling matrix extraction of lossy filters is presented and successfully evaluated using simulated and measured scattering parameter data.**

***Index Terms*—Coupling matrix, coupling matrix extraction, filtering theory, infinitesimal rotation, lossy filters, microwave filters, similarity transform.**

I. Introduction

THE COUPLING matrix is a mathematical filter model that is often employed in modern filter synthesis and analysis procedures. Advanced synthesis methods for coupling matrix descriptions of filters incorporating cross-couplings [1] and losses [2] have been described in the literature. However, these methods often result in coupling matrices with a structure that is inconvenient for hardware implementation. Depending on the technology used, some structures may be more suitable for realization than others. A fully populated coupling matrix, for example, would require direct coupling between all of the resonators. Clearly, this topology is not convenient for realization within, for example, planar microstrip technology. An additional step, transforming the synthesized coupling matrix into a matrix that realizes the same scattering parameters with a simpler topology, is required for reasonable implementation of the filter.

Manuscript received March 10, 2015; revised July 19, 2015 and October 18, 2015; accepted October 23, 2015. Date of publication November 17, 2015; date of current version January 01, 2016. This work was supported in part by the German Federal Ministry of Education and Research under Contract KUSZ 16BU1226. *(Corresponding author: Stefan Pflüger.)*

S. Pflüger and V. Ziegler are with AIRBUS Group Innovations, 81663 Munich, Germany (e-mail: mail@stefanpflueger.info).

C. Waldschmidt is with the Institute of Microwave Techniques, University of Ulm, 89081 Ulm, Germany.

Color versions of one or more of the figures in this paper are available online at http://ieeexplore.ieee.org.

Digital Object Identifier 10.1109/TMTT.2015.2498188

Besides its importance for filter synthesis, finding a transformation step between two arbitrary coupling matrix structures is also of relevance for filter analysis. Following fabrication of a filter, the designer is usually interested in extracting unloaded quality factors and resonator coupling values from measured scattering data. These parameters are essential for filter diagnosis and subsequent filter tuning. A correlation between the entries of a coupling matrix extracted from measurement data and the physical coupling elements of the filter can only be established easily if the coupling matrix is transformed to fit the topology of the filter.

Several methods are known for reconfiguration of fully populated coupling matrices into a better suitable form. These are often based on mathematical similarity transforms that change the coupling values, but leave the eigenstructure of the matrix unaffected. Therefore, these transformations modify the coupling values without influencing the scattering parameters as seen by the I/O ports. Reference [1] gives sequences of transformation steps that transform a general coupling matrix into a specific realizable topology like the folded form or the cul-de-sac configuration. However, the authors of [3] note that it seems that "there is no simple closed form equation" for calculating transformation sequences that transform into any general prescribed structure. In [3], a method is given for exhaustively calculating all possible alternative coupling matrix structures to a given coupling matrix. Whereas this method has the advantage of finding all possible solutions to the problem, the algorithm is computationally highly complex, as it involves symbolic calculation of the matrix inverse of the coupling matrix. Besides analytical solutions, optimization methods are often used. These try to simultaneously meet conditions on the resulting scattering parameters as well as on the topology of the matrix. However, local optimization methods as used in [4] and [5] are not guaranteed to converge to a solution that meets all goals. If the goals cannot be met simultaneously, the results will not match the desired scattering parameters. To avoid convergence to local minima, the authors of [6] have used a genetic algorithm that tries to find a coupling matrix that simultaneously meets the requirements on scattering parameters and structure. Genetic algorithms are successfully used for solving optimization problems with complex boundary conditions, but the time for convergence to a suitable solution can be high.

In this paper, a novel approach for transformation of a general coupling matrix into an arbitrary desired topology is presented in Section II. This new approach avoids direct optimization of the values within the coupling matrix. Instead, the basis of the vector space defined by the coupling matrix is changed iteratively in small steps, i.e., each iteration result is another perspective on the same starting matrix with its given eigenvalues. In each iteration, a gradient can be determined that gradually changes the basis into a direction that better fulfills the desired matrix structure target. As only the matrix basis is changed, there is no accumulation of numerical inaccuracies throughout the iterations.

It is intrinsic to the method that the spectral properties of the matrix and the resulting scattering parameters do not change throughout the iterations. Whereas the referenced direct optimization methods will compromise on the scattering parameter data to meet the given topology goal, the proposed method will give a coupling matrix that realizes the desired scattering parameters exactly and matches the desired structure as good as possible in a least squares sense. This is especially advantageous for coupling matrix extraction if parasitic couplings between resonators have to be considered. Section III focuses on the use of the proposed reconfiguration method for coupling matrix extraction of lossy filters and gives several examples for verification of the method.

II. Reconfiguration of Coupling Matrices

A. Basic Coupling Matrix Model

Throughout this paper, the normalized $N+2$ coupling matrix M is used that includes the I/O coupling values within the matrix. The rows and columns associated with these I/O couplings are marked with a light gray background for better readability of the matrices.

The scattering parameters s_{mn} are given by the normalized impedance matrix Z and can be calculated as

$$s_{mn} = \begin{cases} 2[Z^{-1}]_{l(m),l(n)}, & \text{if } m \neq n \\ 1 - [Z^{-1}]_{l(m),l(n)}, & \text{if } m = n \end{cases} \tag{1}$$

where $l(x)$ maps the xth port to the corresponding line and column in the coupling matrix. The inverse of the matrix Z can be expressed using the adjoint and determinant of Z as [7]

$$Z^{-1} = \frac{\operatorname{adj}(Z)}{\det(Z)}. \tag{2}$$

The impedance matrix Z can be determined from the coupling matrix M with the low-pass frequency domain variable p, $R = \operatorname{diag}(1, 0, \ldots, 0, 1)$, and $I = \operatorname{diag}(0, 1, \ldots, 1, 0)$,

$$Z = R - jM + pI = -j\hat{M} + pI. \tag{3}$$

Within this model, the matrix R in general describes losses and can be combined with the real-valued coupling matrix M to form a complex valued coupling matrix $\hat{M} = M + jR$. For a detailed description of the model and its derivation, see, for example, [2] and [8]–[10].

B. Description of the Reconfiguration Method

An $N+2$ coupling matrix $X \in R^{n \times n}$ is given. Following [11], a projection P is defined that suppresses all undesired matrix entries

$$P(X) := A_0 + S \circ X. \tag{4}$$

The $\circ$ operator denotes the Hadamard elementwise product and S is a binary matrix defining the desired final matrix structure. S contains a zero for each element of X that is desired to vanish in the final reconfigured result and a one for all other elements. Using these definitions, the transformation of X to yield the matrix structure defined by P can be formulated as a minimization problem [11]

$$F(X) := \|X - P(X)\|_{\mathrm{F}}^2 \stackrel{!}{=} \min \tag{5}$$

with the Frobenius norm $\|A\|_{\mathrm{F}}^2 = \operatorname{Tr}(A^T A)$. The scalar function $F(X)$, called the "structure difference" below, can be understood as a measure of how good the coupling matrix X fits the desired structure determined by P.

By using the eigenvalue decomposition theorem, the coupling matrix X can be decomposed into an $N+2$ transversal coupling matrix Λ, also known as a global eigenmode representation [12], and a similarity transformation given by the orthogonal matrix Q as [1]

$$X = Q^T \Lambda Q. \tag{6}$$

The structure difference $F(X)$ in (5) can then be written as

$$F(X) = \|Q^T \Lambda Q - P(Q^T \Lambda Q)\|_{\mathrm{F}}^2. \tag{7}$$

A comprehensive discussion of the concept of similarity transforms within the coupling matrix model can be found in [12].

Instead of directly modifying the matrix X, the proposed optimization approach changes the similarity transformation matrix Q. The location of the filter poles and zeros is invariant with respect to this modification as long as the following two aspects are observed. First of all, the generalized eigenvalues of the matrix pencil (X, I), which are equal to the transmission poles of the filter, must not be changed throughout the transformation. This requirement is fulfilled by definition if Q describes a similarity transformation because similar matrices share the same eigenvalues. Additionally, transmission and reflection zeros also need to remain unchanged by the transformation. The position of these zeros is influenced by the eigenvalues of the corresponding matrix minors, as can be seen by calculating the elements of the adjoint matrix in (2). Hence, the transformations carried out on the submatrices corresponding to these matrix minors are also required to be similarity transforms. These requirements are all met if the transformation matrix Q is chosen as follows with an arbitrary similarity transformation matrix $Q^{\square}$:

$$Q = \begin{bmatrix} 1 & 0 & \ldots & 0 & 0 \\ 0 & & & & 0 \\ \vdots & & Q^{\square} & & \vdots \\ 0 & & & & 0 \\ 0 & 0 & \ldots & 0 & 1 \end{bmatrix}. \tag{8}$$

It is assumed that the first and last rows and columns of the $N+2$ coupling matrix X describe the input and output ports of the filter. The corresponding elements of Q have been marked gray in (8). These have been set to 0, except for the diagonal elements, which have been set to 1. This avoids transformations involving the outer matrix elements, as this would change the eigenvalues of the matrix minors and thereby change the filter zeros as stated before. As long as Q fulfills the condition shown, the filter poles and zeros automatically remain unchanged throughout the minimization process.

The scalar function $F(X)$ is to be minimized. To simplify the following calculations, the matrix Q is first multiplied by the term $r = (I + e)$ with the identity matrix I and an antisymmetric matrix e with infinitesimally small elements. Note that the term $(I + e)$ is equivalent to the description of an additional infinitesimal rotation if $e = -e^T$ [13]. Adding an infinitesimal rotation does not affect the orthogonality of Q. As discussed before, this is a desired property for the minimization of $F(X)$. Thus, this condition shall be assumed to hold true below.

The optimization problem of (5) can then be stated as

$$F(X) = \|r^T Q^T \Lambda Q r - P(r^T Q^T \Lambda Q r)\|_{\mathrm{F}}^2. \tag{9}$$

The partial derivatives of $F(X)$ with respect to the infinitesimal rotations found in the matrix elements $e_{i,j}$ of e can then be calculated as

$$\frac{\partial F(X)}{\partial e_{i,j}} = \frac{\partial \|X - P(X)\|_{\mathrm{F}}^2}{\partial e_{i,j}} \tag{10}$$

$$= \mathrm{Tr}\left[(\frac{\partial \|X\|_{\mathrm{F}}^2}{\partial X})^T \cdot \frac{\partial (X - P(X))}{\partial e_{i,j}} \right] \tag{11}$$

$$= \mathrm{Tr}\Bigg[2(Q^T \Lambda Q - P(Q^T \Lambda Q)) \cdot \left(\frac{\partial r^T Q^T \Lambda Q r}{\partial e_{i,j}} - \frac{\partial P(r^T Q^T \Lambda Q r)}{\partial e_{i,j}} \right) \Bigg]. \tag{12}$$

The remaining derivative terms in this expression can be written as follows using the single entry matrix $J^{i,j}$ [7]:

$$\frac{\partial P(X)}{\partial e_{i,j}} = S \circ \frac{\partial X}{\partial e_{i,j}} \tag{13}$$

$$\frac{\partial r^T Q^T \Lambda Q r}{\partial e_{i,j}} = Q^T \Lambda Q J^{i,j} - J^{i,j} Q^T \Lambda Q. \tag{14}$$

Replacing the derivative terms in (12) by the results shown in (13)–(14) finally gives the following expression for the partial derivatives of $F(X)$:

$$\frac{\partial F(X)}{\partial e_{i,j}} = 2\mathrm{Tr}[(X - P(X)) \cdot (V - S \circ V)] \tag{15}$$

with the matrix V defined as

$$V := Q^T \Lambda Q J^{i,j} - J^{i,j} Q^T \Lambda Q. \tag{16}$$

Using the partial derivatives given by (15), the gradient of F with respect to an infinitesimal rotation matrix e can be written as

$$g_{i,j} = \frac{\partial F(X)}{\partial e_{i,j}} - \frac{\partial F(X)}{\partial e_{j,i}}. \tag{17}$$

The subtraction of the second term in (17) is due to the antisymmetric structure [7] of the matrix e.

Subsequently, with the gradient known, the gradient descent method can be employed to follow the gradient to a solution of the minimization problem. During this process, the transformation matrix Q needs to keep the structure defined by (8) with $Q^{\square}$ being an orthogonal matrix. The orthogonality property is not affected by adding infinitesimal rotation steps as shown before. To keep the outer values of Q fixed, as described in (8), the boundary elements of the gradient matrix in (17) are set to zero. With these considerations, the gradient descent method can be formulated by the iteration

$$Q^{(i+1)} = Q^{(i)} \cdot (I - \delta g) = Q^{(i)} - \delta Q^{(i)} g \tag{18}$$

with δ small enough and a given starting point $Q^{(0)}$. A possible starting point is the identity matrix $Q^{(0)} = I$. With this choice, $\Lambda = X$ is directly known without any prior calculations as can be seen from (6).

The expressions in (18) lead to two different interpretations of the algorithm. The first expression, $Q^{(i+1)} = Q^{(i)} \cdot (I - \delta g)$, can be understood to describe a sequence of infinitesimally small rotations $(I - \delta g)$ that are applied to move towards the optimization goal. In the limit of infinitesimally small steps, these rotations then describe a continuous path from the starting point to the final optimization goal. From this perspective, the algorithm proposed in this work can be seen as a continuous analogy to the discrete rotation steps of the well-known classical similarity transformations. Following the transformation path continuously is advantageous for a robust optimiziation algorithm because, contrary to classical matrix rotations, the order in which subsequent infinitesimal rotation steps are applied is not relevant for the result [13]. The second expression, $Q^{(i+1)} = Q^{(i)} - \delta Q^{(i)} g$, gives rise to an interpretation of the algorithm in terms of a vector field $Q^{(i)} g$. Each step along the direction of this vector field moves the algorithm further towards the optimization goal while retaining the spectral properties—the poles and zeros—of the underlying coupling matrix. A particle starting at the initial point and flowing along the direction of this vector field would eventually reach the optimization goal. As such, the algorithm is similar to the isospectral flows, which are discussed in [11], for example.

In general, choosing a sufficiently small step size δ leads to a solution, but results in a considerable number of iterations. To speed up the algorithm, we chose to select δ adaptively. After each iteration step, the structure difference $F(X)$ is evaluated. If $F(X)$ did not decrease with respect to the previous iteration, the iteration is continued from the previous step with smaller δ. If δ is not infinitesimally small, the application of (18) will cause a loss of orthogonality between the columns of the matrix Q. If δ is chosen small enough, this effect can be neglected, accepting a small error in the final result. However, when selecting δ adaptively and not necessarily small, the orthogonality of the matrix Q needs to be restored. This has been accomplished by subsequent application of the Gram–Schmidt orthonormalization procedure on the columns of $Q^{(i+1)}$. Additionally, (18) followed by the Gram–Schmidt algorithm can be applied multiple times without recalculation of the gradient to speed up the algorithm further.

Algorithm 1 summarizes the steps of the reconfiguration method using a pseudo-code notation.

$$M = \begin{bmatrix} 0 & 0.3641 & -0.6537 & 0.6677 & -0.3433 & 0.0151 \\ 0.3641 & 1.3142 & 0 & 0 & 0 & 0.3641 \\ -0.6537 & 0 & 0.7831 & 0 & 0 & 0.6537 \\ 0.6677 & 0 & 0 & -0.8041 & 0 & 0.6677 \\ -0.3433 & 0 & 0 & 0 & -1.2968 & 0.3433 \\ 0.0151 & 0.3641 & 0.6537 & 0.6677 & 0.3433 & 0 \end{bmatrix}$$

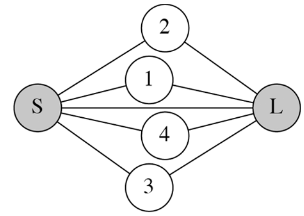

$$M_{fold} = \begin{bmatrix} 0 & 1.06 & 0 & 0 & 0 & 0.0151 \\ 1.06 & -0.0022 & 0.8739 & 0 & -0.3259 & 0.0313 \\ 0 & 0.8739 & 0.0483 & 0.836 & 0.0342 & 0 \\ 0 & 0 & 0.836 & -0.0668 & 0.8723 & 0 \\ 0 & -0.3259 & 0.0342 & 0.8723 & 0.0171 & 1.0595 \\ 0.0151 & 0.0313 & 0 & 0 & 1.0595 & 0 \end{bmatrix}$$

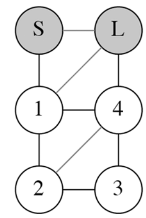

Fig. 1. Initial coupling matrix M and reconfigured coupling matrix M_{fold} in folded form of example 1.

Algorithm 1 Steps of the reconfiguration algorithm in pseudocode notation.

$Q :=$ identity matrix

$\Lambda :=$ matrix to reconfigure

repeat

score1 $:= F(Q^T \Lambda Q)$, see **(5)**

$g :=$ Gradient matrix given by **(15)** and **(17)**

$Q := Q(I - \delta g)$

$Q :=$ GramSchmidt(Q)

score2 $:= F(Q^T \Lambda Q)$, see **(5)**

if score2 $\geq$ score1 **then**

Decrease value of δ

Continue loop from previous step

end if

until score2 $<$ limit or $\delta <$ limit

C. Examples

1) Example 1: To demonstrate the application of the method, the transversal coupling matrix from [1], shown in Fig. 1, is used. This matrix describes a fully canonical filter with four transmission poles and four transmission zeros. This coupling matrix shall be reconfigured into the folded form [1] that is given by the following structure matrix:

$$S = \begin{bmatrix} 0 & 1 & 0 & 0 & 0 & 1 \\ 1 & 1 & 1 & 0 & 1 & 1 \\ 0 & 1 & 1 & 1 & 1 & 0 \\ 0 & 0 & 1 & 1 & 1 & 0 \\ 0 & 1 & 1 & 1 & 1 & 1 \\ 1 & 1 & 0 & 0 & 1 & 0 \end{bmatrix}. \tag{19}$$

The iterative optimization algorithm described before has been applied to this example. The matrix to be reconfigured is set to $\Lambda = M$, the matrices M and S are shown in Fig. 1. The identity matrix has been chosen as initial transformation matrix Q. Q is the only matrix that changes during the iterations of the algorithm, Λ and S are not modified in any way. The step size δ has been constant with $\delta = 0.01$ for this example. To provide a reference for implementation, the matrix g within the first iteration step is shown,

$$g_{(1)} = \begin{bmatrix} 0 & 0 & 0 & 0 & 0 & 0 \\ 0 & 0 & 0 & 0.9724 & -0.25 & 0 \\ 0 & 0 & 0 & 0 & 0.4488 & 0 \\ 0 & -0.9724 & 0 & 0 & -0.4584 & 0 \\ 0 & 0.25 & 0.4488 & 0.4584 & 0 & 0 \\ 0 & 0 & 0 & 0 & 0 & 0 \end{bmatrix}$$

Using the transformation matrices $Q_{(n)}$ of the subsequent iterations, the concept of eigenvalue conservation during the reconfiguration process can be demonstrated. The finite generalized eigenvalues of the matrix pencil $(Q_{(0)}^T \Lambda Q_{(0)}, I) = (\Lambda, I)$, i.e., the solutions to the equation $\det(\Lambda - \lambda_i I) = 0$, can be calculated as

$$\lambda_{(0)} = [-1.2030 + 0.2032j \quad 1.2058 + 0.2272j \quad 0.7058 + 0.8868j \quad -0.7132 + 0.9292j].$$

These eigenvalues are found to be equal to the filter poles, as has been explained in Section II. After completing the first iteration step, the eigenvalues of the pencil $(Q_{(1)}^T \Lambda Q_{(1)}, I)$ are found to be unchanged,

$$\lambda_{(1)} = [-1.2030 + 0.2032j \quad 1.2058 + 0.2272j \quad 0.7058 + 0.8868j \quad -0.7132 + 0.9292j].$$

It can be seen from the plot of the absolute value of the difference between the eigenvalue vectors of the first and the nth iteration in Fig. 2 that the eigenvalues remain invariant throughout all iterations. The same is true for the eigenvalues of the matrix minors, which determine the zeros of the filter transfer functions, as has been explained in Section II. Additionally, the eigenvalue variation plot in Fig. 2 demonstrates that small numeric errors caused by limited machine precision and finite step size δ do not add up throughout the iterations. For more information about eigenvalue decompositions in the

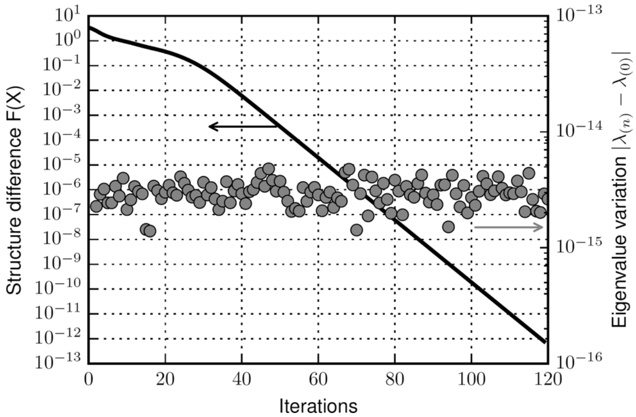

Fig. 2. Convergence behavior of the algorithm shown in terms of structure difference $F(X)$ and variation of the eigenvalues over number of iterations.

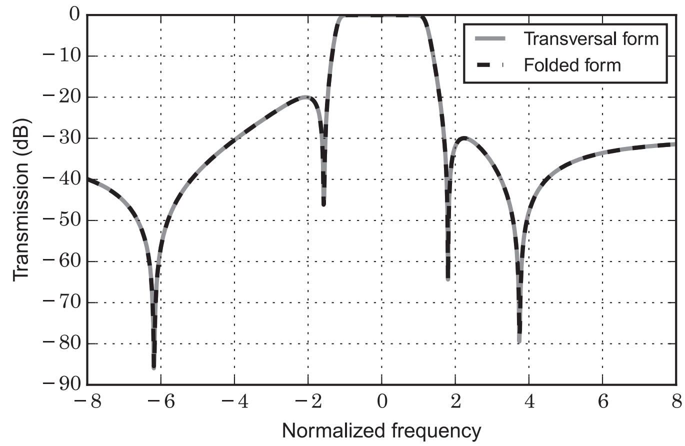

Fig. 3. Comparison of scattering parameter magnitude $|s_{21}|$ of original matrix in transversal form and after transformation to folded form.

context of coupling matrices, the reader shall be referred to [12] for further reading.

For the example shown, the optimization process has been continued until the structure difference $F(X)$ defined in (5) was smaller than a limit of 10^{-12}. The convergence behavior of the minimization in terms of the structure difference $F(X)$ is plotted in Fig. 2. The algorithm has been implemented using the Python scripting language, calculation took 0.31 s of time on an Intel Core i5 processor with 2.4 GHz. The resulting coupling matrix $\hat{M}_{\text{fold}}$ after reaching the stopping criterion is given in Fig. 1.

The transformation from transversal to folded form has been deliberately chosen as an example because it is one of the special cases where a sequence of classical similarity transforms can be given explicitly to solve the problem. Therefore, the results of the proposed algorithm can easily be compared to the results of the classical similarity transforms that are well documented in the literature. In [1], this known sequence of similarity transforms has been used to derive the solution. The solution given there is identical to the solution derived by the method shown in this work for all decimal places given. A comparison of the scattering parameters of the original transversal coupling matrix and the reconfigured coupling matrix in folded form is shown in Fig. 3. The excellent agreement between the scattering parameters of the original matrix in transversal form and the transformed matrix in folded form shows the validity of the method.

2) Example 2: To demonstrate the applicability of the proposed method for more complex filter structures, a transformation from arrow form to a ten-pole extended box topology has been chosen. The coupling matrix in arrow form, which has been generated using the methods included in Dedale-HF [14] from given poles and zeros, is shown in Fig. 4. This matrix is to be transformed into the ten-pole extended box topology described by the structure matrix that is as well printed in Fig. 4. In general, there may be multiple solutions to the reconfiguration problem that are identical in terms of poles and zeros of the filter. The conditions required for a coupling matrix reconfiguration problem to possess a unique, multiple, or even an infinite number of solutions has been assessed in [3]. From this work, it is known that the extended box topology chosen for this example has a total number of 384 distinct complex solutions.

The algorithm proposed in this work is based on gradient optimization. The optimization problem in the example is ill posed in the sense that is has multiple solutions. Therefore, the convergence to a specific solution depends upon the starting point of the optimization. Instead of starting the algorithm with Q equal to the identity matrix, the initial transformation matrix Q has been chosen as a sequence of random matrix rotations $Q_{i,j}$ to discover multiple solutions

$$Q = \prod_{i=2}^{N-1} \prod_{j=i+1}^{N-1} Q_{ij} \tag{20}$$

with $Q_{i,j}$ defined as the transformation matrix

$$\begin{array}{cc} & \begin{array}{ccccc} & i & & j & \end{array} \\ \begin{array}{c} \\ i \\ \\ j \\ \\ \end{array} & \begin{pmatrix} 1 & 0 & \dots & 0 & 0 \\ 0 & \cos(\phi_r) & 0 & -\sin(\phi_r) & 0 \\ \vdots & 0 & 1 & 0 & \vdots \\ 0 & \sin(\phi_r) & 0 & \cos(\phi_r) & 0 \\ 0 & 0 & \dots & 0 & 1 \end{pmatrix} \end{array} = Q_{ij}. \tag{21}$$

To study the properties of the the proposed coupling matrix reconfiguration algorithm, this procedure has been repeated 10.000 times with the randomly transformed starting point Q. In 47% of these runs an exact solution to the reconfiguration problem has been found. Fig. 5 depicts a histogram of the number of runs that converged to a solution within a given number of iterations. On average, it took 10 294 iterations for the algorithm to converge to a solution.

To validate the results, a comparison with the software package Dedale-HF [14] has been carried out. Dedale-HF is able to determine the solution set of the coupling matrix reconfiguration problem exhaustively by symbolic calculation. The authors of Dedale-HF have found a way of pre-calculating the results of the time-consuming symbolic matrix inversion and storing the results in a reference file that is specific to a given filter topology. As soon as this reference file has been created, further calculations for the specific filter topology can be carried out within little time.

For the ten-pole extended box topology, a total number of 384 solutions exist, not including sign symmetries [3]. Using Dedale-HF, it has been found that for the example considered in this section, 44 out of these 384 solutions, have a real-valued

$$S=\begin{bmatrix}0&1&0&0&0&0&0&0&0&0&0&0\\1&1&1&0&1&0&0&0&0&0&0&0\\0&1&1&1&0&0&0&0&0&0&0&0\\0&0&1&1&1&0&1&0&0&0&0&0\\0&1&0&1&1&1&0&0&0&0&0&0\\0&0&0&0&1&1&1&0&1&0&0&0\\0&0&0&1&0&1&1&1&0&0&0&0\\0&0&0&0&0&0&1&1&1&0&1&0\\0&0&0&0&0&1&0&1&1&1&0&0\\0&0&0&0&0&0&0&0&1&1&1&0\\0&0&0&0&0&0&0&1&0&1&1&1\\0&0&0&0&0&0&0&0&0&0&1&0\end{bmatrix}$$

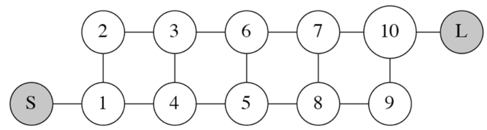

$$M_0=\begin{bmatrix}0&1&0&0&0&0&0&0&0&0&0&0\\1&0.0026&-0.8534&0.0000&0.0000&0.0000&0.0000&0.0000&0.0000&0.0000&0.0000&0\\0&-0.8534&0.0027&-0.5926&0.0000&0.0000&0.0000&0.0000&0.0000&0.0000&0.0000&0\\0&0.0000&-0.5926&0.0030&-0.5456&0.0000&0.0000&0.0000&0.0000&0.0000&0.0000&0\\0&0.0000&0.0000&-0.5456&0.0039&-0.5302&0.0000&0.0000&0.0000&0.0000&0.0000&0\\0&0.0000&0.0000&0.0000&-0.5302&0.0085&-0.5222&0.0000&0.0000&0.0000&0.0950&0\\0&0.0000&0.0000&0.0000&0.0000&-0.5222&-0.0598&-0.4247&0.0000&0.0000&-0.3623&0\\0&0.0000&0.0000&0.0000&0.0000&0.0000&-0.4247&-0.0205&-0.7622&0.0000&0.0975&0\\0&0.0000&0.0000&0.0000&0.0000&0.0000&0.0000&-0.7622&0.2352&-0.1398&0.6661&0\\0&0.0000&0.0000&0.0000&0.0000&0.0000&0.0000&0.0000&-0.1398&-0.9626&-0.3672&0\\0&0.0000&0.0000&0.0000&0.0000&0.0950&-0.3623&0.0975&0.6661&-0.3672&0.0026&1\\0&0&0&0&0&0&0&0&0&0&1&0\end{bmatrix}$$

Fig. 4. Structure matrix S and initial coupling matrix M in folded form of the ten-pole extended box example.

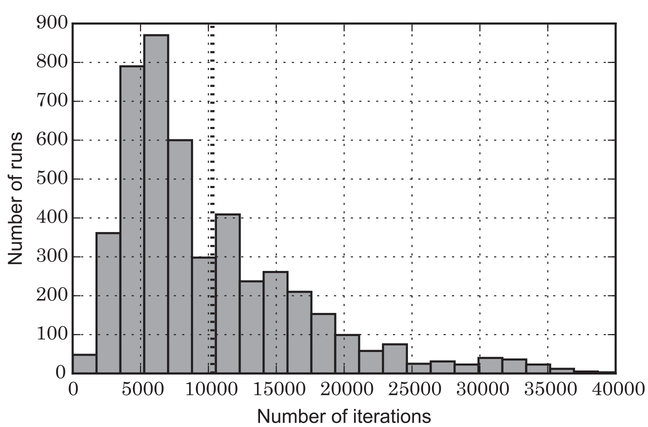

Fig. 5. Histogram of the number of runs out of 10.000 runs that completed within a given range of iterations for the ten-pole extended box reconfiguration problem.

coupling matrix solution, which is required for physical implementation. These solutions have been compared with the results of the proposed reconfiguration method. All exact solutions found by Dedale-HF also have been found using the method proposed in this work, which does not require the complex creation of a reference file and is comparatively easy to implement.

There is a remaining number of runs that did not converge to an exact solution. The solution set of these runs includes solutions that do not exactly reach the desired filter topology, but are near optimum in terms of the structure difference criterion stated in (5). These solutions cannot be found using the approach taken by Dedale-HF, but might also be considered for filter implementation, if small deviations from the requested scattering parameters are still within the filter specification.

Examples of how it is useful to be able to find non-exact, but optimum solutions in terms of (5) are shown in Section III within the application of coupling matrix extraction.

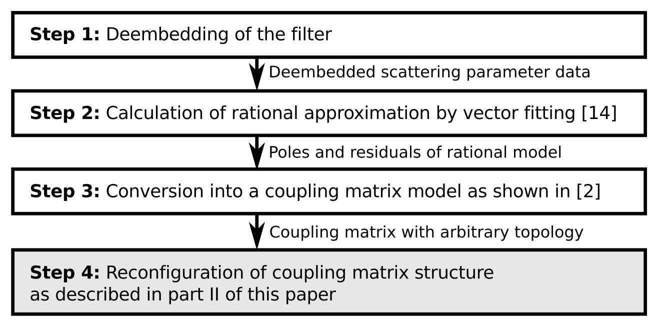

Fig. 6. Process of coupling matrix extraction from scattering parameter data, extending the method proposed in [2].

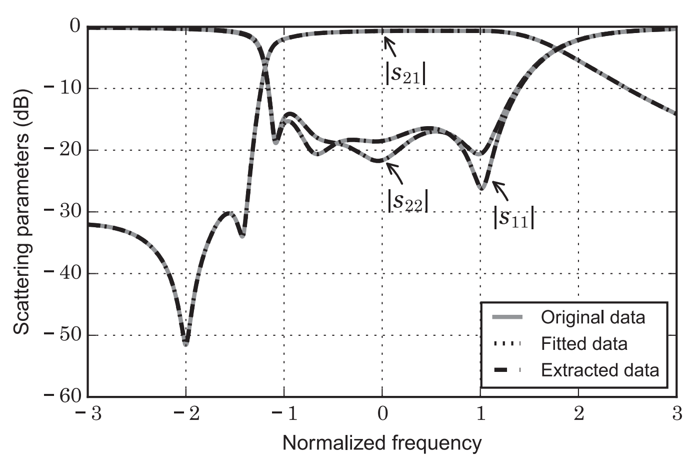

Fig. 7. Comparison of the original set of scattering parameters to the result of vector fitting and the scattering parameters calculated from the extracted coupling matrix.

III. Coupling Matrix Extraction

As outlined in Section I, there are many fields of application for the reconfiguration algorithm presented in Section II. In combination with the synthesis procedure shown in [2], the

$$\hat{M} = \begin{bmatrix} -1j & 1.1 & 0 & 0 & 0 & 0 \\ 1.1 & 0.155-0.05j & -0.3 & -0.9 & -0.35 & 0.0 \\ 0 & -0.3 & -1.1-0.04j & 0 & -0.3 & 0 \\ 0 & -0.9 & 0 & 0-0.04j & 1 & 0 \\ 0 & -0.35 & -0.3 & 1 & 0.15-0.05j & 1.1 \\ 0 & 0 & 0 & 0 & 1.1 & -1j \end{bmatrix}$$

$$\hat{M}_{extracted} = \begin{bmatrix} -1j & 1.1 & 0 & 0 & 0 & 0 \\ 1.1 & 0.155-0.050j & 0.350-0.000j & -0.940-0.000j & -0.130+0.004j & 0 \\ 0 & 0.350-0.000j & 0.150-0.050j & -0.928+0.002j & 0.478+0.004j & 1.1 \\ 0 & -0.940-0.000j & -0.928+0.002j & -0.037-0.041j & -0.198-0.004j & 0 \\ 0 & -0.130+0.004j & 0.478+0.004j & -0.198-0.004j & -1.063-0.039j & 0 \\ 0 & 0 & 1.1 & 0 & 0 & -1j \end{bmatrix}$$

$$\hat{M}_{transformed} = \begin{bmatrix} -1j & 1.1 & 0 & 0 & 0 & 0 \\ 1.1 & 0.155-0.050j & 0.300-0.003j & -0.900-0.001j & 0.350-0.000j & 0 \\ 0 & 0.300-0.003j & -1.100-0.040j & 0.000+0.004j & -0.300-0.004j & 0 \\ 0 & -0.900-0.001j & 0.000+0.004j & 0.000-0.040j & -1.000+0.001j & 0 \\ 0 & 0.350-0.000j & -0.300-0.004j & -1.000+0.001j & 0.150-0.050j & 1.1 \\ 0 & 0 & 0 & 0 & 1.1 & -1j \end{bmatrix}$$

Fig. 8. Coupling matrix $\hat{M}$ used to generate scattering parameters for validation of the algorithm, coupling matrix extracted from these scattering parameters ($\hat{M}_{\text{extracted}}$), and coupling matrix transformed into the desired topology ($\hat{M}_{\text{transformed}}$).

calculation of a coupling matrix with desired structure from a rational function description of a general lossy filter is possible. This rational function description of the admittance parameters of the filter can be derived from scattering parameter data by transformation to Y-parameters followed by rational approximation.

Recently, the vector-fitting algorithm has gained attention for rational approximation within different fields of engineering science. In [15], vector fitting has been used successfully to extract a rational model from measured admittance parameter data for use in computer-aided tuning of lossy filters. The vector fitting algorithm [16] has been found to give reliable results for rational approximation with order N and has also been used in the example given below. As the rational function model with low order is unable to model a time delay at the filter ports, any potential time delay first has to be deembedded from the ports, as is also suggested in [17]. The order N of the fit has to be chosen equal to the order of the coupling matrix model to be calculated from the synthesis procedure. The quality of the fit can be used as an indicator whether or not the given scattering parameter data can be described by a coupling matrix representation of order N.

This procedure is summarized in Fig. 6 in Steps 1–3. Generally, the result is a fully populated coupling matrix with complex values. The real part of these values describe classical capacitive and inductive coupling between the resonators, as well as self-coupling. Imaginary values on the diagonal entries describe losses within the resonator that can be related to an unloaded quality factor. The interpretation of imaginary values in off-diagonal matrix entries is discussed in [2] and [18].

The structure of the complex coupling matrix resulting from Step 3 of the process usually does not reflect the topology of the real filter being measured. To correlate the values of the extracted coupling matrix with the parameters of the measured filter, the coupling matrix first needs to be transformed to reflect the topology of the filter. This is achieved in Step 4 using the coupling matrix reconfiguration algorithm presented before.

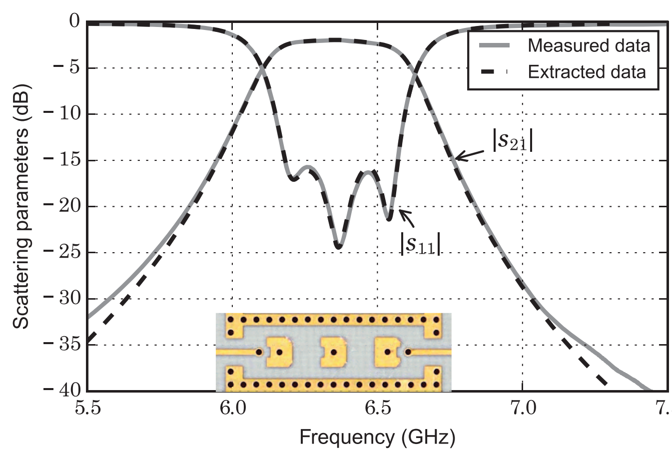

Fig. 9. Comparison of magnitudes of original scattering parameters and measured scattering parameters of a three-pole filter. A photograph of this filter is shown at the bottom of the graph.

Below, the validity of this coupling matrix extraction process shall be demonstrated using two examples. The first example uses scattering parameter data generated from a given coupling matrix model to assess the accuracy of the approach. The second example uses measured data of a planar filter to demonstrate the ability of the procedure to deal with the imperfections of real data.

A. Evaluation of Accuracy

To validate the extraction process shown in Fig. 6, a set of scattering parameters has been calculated by applying (1) to a known complex lossy coupling matrix $\hat{M}$ that represents a four-pole asymmetric filter with two transmission zeros near the passband edge. The corresponding scattering parameters are

$$\hat{M}_{transformed} = \begin{bmatrix} -1j & 0.077 & 0.832 & 0.022 & -0.001 & 0 & 0.001 \\ 0.077 & -1j & 0 & 0 & 0 & 0 & 0 \\ 0.832 & 0 & 0.312 - 0.110j & -0.684 + 0.001j & 0.027 + 0.002j & 0 & -0.002 \\ 0.022 & 0 & -0.684 + 0.001j & 0.260 - 0.098j & 0.699 + 0.000j & 0 & 0.022 \\ -0.001 & 0 & 0.027 + 0.002j & 0.699 + 0.000 & 0.234 - 0.107j & 0 & -0.847 \\ 0 & 0 & 0 & 0 & 0 & -1j & 0.054 \\ 0.001 & 0 & -0.002 & 0.022 & -0.847 & 0.054 & -1j \end{bmatrix}$$

Fig. 10. Coupling matrix extracted from measured scattering parameters.

shown in Fig. 7 using a solid gray line. Fig. 8 shows the coupling matrix $\hat{M}$. The filter topology is similar to the example given in [2].

Fitting the scattering parameters of the filter using the vector fitting algorithm (Step 1) and converting the resulting rational model to a coupling matrix model as described before results in the fully populated coupling matrix shown in Fig. 8. The scattering parameters derived from this coupling matrix match the original set of scattering parameters very well, as is shown in Fig. 7. However, the matrix structure of the extracted coupling matrix is substantially different to the original matrix $\hat{M}$, particularly with regard to the coupling between the second and third resonators. There is significant coupling between these resonators in the extracted coupling matrix although there is no direct coupling between these two resonators in the original filter topology.

To be able to compare the coupling values within these two coupling matrices, the reconfiguration process derived in this paper has been carried out. The real part of $\hat{M}_{\text{extracted}}$, describing the coupling structure, has been used as input for the reconfiguration algorithm. The resulting transformation matrix Q has subsequently been applied to the complex matrix in Fig. 8 including losses by calculating

$$\hat{M}_{\text{transformed}} = Q^T \cdot \hat{M}_{\text{extracted}} \cdot Q. \tag{22}$$

Hereby, the extracted lossy coupling matrix can be transformed into the coupling structure of the original coupling matrix. The result of this transformation is shown in Fig. 8. The coupling matrix values match the values of the original matrix $\hat{M}$ closely.

B. Extraction From Measured Scattering Parameters

The ability to reconfigure an arbitrary coupling matrix to yield a prescribed structure has been found especially useful for the extraction of unloaded quality factors as well as coupling values from measured scattering parameters of filters.

A filter based on three transversally coupled evanescent-mode resonators is used to demonstrate this application. The basic structure of this filter has been described before in [19]. A photograph of the filter is shown in Fig. 9. Essentially, a substrate integrated waveguide is formed using a via fence. This waveguide is operated below its cutoff frequency. By capacitively loading the evanescent waveguide at three places, three resonators are formed. These are coupled by the evanescent fields extending into the waveguide. Measured scattering parameters of the filter are shown in Fig. 9. For a better overview, only the scattering parameters s_{21} and s_{11} are shown in this figure. Nonetheless, the full set of scattering parameters has been used for analysis of the filter.

The analysis has been carried out by following the steps shown in Fig. 6 and described above. The target structure of the coupling matrix reconfiguration (Step 4) has been chosen to represent a transversally coupled filter without cross-couplings,

$$S = \begin{bmatrix} 0 & 1 & 1 & 0 & 0 & 0 & 0 \\ 1 & 0 & 0 & 0 & 0 & 0 & 0 \\ 1 & 0 & 1 & 1 & 0 & 0 & 0 \\ 0 & 0 & 1 & 1 & 1 & 0 & 0 \\ 0 & 0 & 0 & 1 & 1 & 0 & 1 \\ 0 & 0 & 0 & 0 & 0 & 0 & 1 \\ 0 & 0 & 0 & 0 & 1 & 1 & 0 \end{bmatrix}. \tag{23}$$

A non-resonant node, which is only coupled to the I/O ports, has been added to the model. The position of the corresponding coupling coefficients is marked with dark gray color in (23). These lossy non-resonant nodes add a shunt conductance [2], which allows the model to include additional losses at the ports. These may originate from an additional lossy transmission line used, for example, during measurement. Throughout the coupling matrix reconfiguration algorithm, these non-resonant nodes are handled in the same way as the I/O ports.

The result of the extraction process is shown in Fig. 10. Before processing of the data, it has been transformed from the bandpass domain into the low-pass domain with a center frequency of $f_0 = 6$ GHz and $\Delta f = 500$ MHz. Therefore, all values within the coupling matrix $\hat{M}_{\text{transformed}}$ are normalized and can be unnormalized by a multiplication with the factor $\Delta f / f_0$. The transversal coupling topology is clearly visible within the matrix in the secondary diagonal entries. Additionally, a slightly varying frequency offset between the resonators can be seen in the main diagonal matrix entries. If this frequency offset was not desired in the filter design, it could now be compensated for by post-production tuning. Knowing the magnitude and location of the deviation from the extracted coupling matrix facilitates this task.

In addition, the unloaded quality factors of the resonators can be derived from this coupling matrix description

$$Q_{u,i} = -\frac{1}{\text{Im}\{M_{i,i}\}} \cdot \frac{f_0}{\Delta f}. \tag{24}$$

By measurement of a single weakly coupled resonator, the unloaded quality factor has been estimated as $Q_u = 127$. For comparison, the unloaded quality factor $Q_{u,2} = 129$ of the inner resonator derived from the coupling matrix of the full filter is in excellent agreement with this result. The extracted values $Q_{u,1} = 115$ and $Q_{u,3} = 118$ of the outer resonators show a slightly lower quality factor, which is most certainly caused by the coupling structures at the outer ports extending into these resonators.

The cross-coupling values in the extracted matrix can be found to be non-zero, which can be plausibly explained by remaining evanescent fields within the waveguide that extend beyond the neighboring resonators. The calculation of these values is the result of a useful property of the proposed reconfiguration algorithm. In the first place, the algorithm ensures that the scattering parameters do not change throughout the reconfiguration. If the desired topology cannot be reached without compromising the scattering parameters, an optimized structure with respect to the least squares criterion defined in (5) is returned.

IV. Conclusion and Outlook

Within this work, an algorithm for reconfiguration of lossy coupling matrices with arbitrary topology has been proposed. Using several examples for verification, the applicability for lossy asymmetric filters has been demonstrated. The concept of infinitesimal rotations as an analog to the classical similarity transformations has been discussed as a foundation of the algorithm.

Furthermore, the proposed algorithm has been used as an integral part of a process for coupling matrix extraction from scattering parameter measurement data of lossy filters. This process is able to extract coupling matrices whose matrix structure resembles the filter topology. As discussed within the paper, this property could enable the use of the coupling matrix extraction process for a wide range of applications including fast filter optimization during filter design as well as manual or automated post-production tuning. The coupling matrix extraction process has as well been successfully demonstrated and verified using simulation and measurement data of a lossy filter.

As has been demonstrated using an example, the mathematical foundation of the method can be generalized to additional non-resonant nodes. It is expected that the method can also be generalized to filters with more than two ports. This would allow its use for further research in optimization of coupling matrices describing multi-port resonant structures.

References

[1] R. J. Cameron, "Advanced coupling matrix synthesis techniques for microwave filters," *IEEE Trans. Microw. Theory Techn.*, vol. 51, no. 1, pp. 1–10, Jan. 2003.

[2] V. Miraftab and M. Yu, "Generalized lossy microwave filter coupling matrix synthesis and design using mixed technologies," *IEEE Trans. Microw. Theory Techn.*, vol. 56, no. 12, pp. 3016–3027, Dec. 2008.

[3] R. J. Cameron, J.-C. Faugere, F. Rouillier, and F. Seyfert, "An exhaustive approach to the coupling matrix synthesis problem application to the design of high degree asymmetric filters," *Int. J. RF Microw. Comput.-Aided Eng.*, vol. 17, no. 1, pp. 4–12, Jan. 2007.

[4] W. Atia, K. Zaki, and A. Atia, "Synthesis of general topology multiple coupled resonator filters by optimization," in *IEEE MTT-S Int. Microw. Symp. Dig.*, Jun. 1998, vol. 2, pp. 821–824.

[5] S. Amari, "Synthesis of cross-coupled resonator filters using an analytical gradient-based optimization technique," *IEEE Trans. Microw. Theory Techn.*, vol. 48, no. 9, pp. 1559–1564, Sep. 2000.

[6] M. Uhm, S. Nam, and J. Kim, "Synthesis of resonator filters with arbitrary topology using hybrid method," *IEEE Trans. Microw. Theory Techn.*, vol. 55, no. 10, pp. 2157–2167, Oct. 2007.

[7] K. B. Petersen and M. S. Pedersen, "The matrix cookbook," Nov. 2012.

[8] A. Atia, A. Williams, and R. Newcomb, "Narrow-band multiple-coupled cavity synthesis," *IEEE Trans. Circuits Syst.*, vol. CAS-21, no. 5, pp. 649–655, Sep. 1974.

[9] R. J. Cameron, "General coupling matrix synthesis methods for Chebyshev filtering functions," *IEEE Trans. Microw. Theory Techn.*, vol. 47, no. 4, pp. 433–442, Apr. 1999.

[10] J.-S. Hong and M. J. Lancaster, *Microstrip Filters for RF/Microwave Applications*. New York, NY, USA: Wiley, 2001.

[11] M. T. Chu and K. R. Driessel, "The projected gradient method for least squares matrix approximations with spectral constraints," *SIAM J. Numer. Anal.*, vol. 27, no. 4, pp. 1050–1060, 1990.

[12] S. Amari and M. Bekheit, "Physical interpretation and implications of similarity transformations in coupled resonator filter design," *IEEE Trans. Microw. Theory Techn.*, vol. 55, no. 6, pp. 1139–1153, Jun. 2007.

[13] E. W. Weisstein, "Infinitesimal rotation," MathWorld—A Wolfram Web Resource [Online]. Available: http://mathworld.wolfram.com/InfinitesimalRotation.html

[14] Dedale-HF v1.3c. INRIA, Sophia Antipolis, France, 2006 [Online]. Available: http://www-sop.inria.fr/apics/Dedale/

[15] H. Hu and K.-L. Wu, "A generalized coupling matrix extraction technique for bandpass filters with uneven-QS," *IEEE Trans. Microw. Theory Techn.*, vol. 62, no. 2, pp. 244–251, Feb. 2014.

[16] B. Gustavsen and A. Semlyen, "Rational approximation of frequency domain responses by vector fitting," *IEEE Trans. Power Del.*, vol. 14, no. 3, pp. 1052–1061, Jul. 1999.

[17] Z. Hao and G. Shi, "New approaches to interconnect macromodeling with explicit delay extraction," in *IEEE Asia–Pacific Circuits Syst. Conf.*, 2008, pp. 1546–1549.

[18] V. Miraftab and M. Yu, "Advanced coupling matrix and admittance function synthesis techniques for dissipative microwave filters," *IEEE Trans. Microw. Theory Techn.*, vol. 57, no. 10, pp. 2429–2438, Oct. 2009.

[19] S. Pflüger, C. Waldschmidt, and V. Ziegler, "Coupled evanescent mode resonator filter using a defective ground structure to increase coupling," in *44th Eur. Microw. Conf.*, Rome, Italy, Oct. 6–9, 2014, pp. 841–844.

Stefan Pflüger received the Dipl.-Ing. degree (with honors) in information technology from the University of Ulm, Ulm, Germany, in 2011, and is currently working toward the Ph.D. degree at the University of Ulm.

From 2006 to 2010, along with his studies, he was with Daimler AG, Ulm, Germany, where he was involved in the area of wireless telematic systems. From 2011 to 2012, he was with the Endress+Hauser GmbH+Co. KG, Maulburg, Germany, where he was involved in the development of radar-based level measurement sensors. Since May 2012, he has been with AIRBUS Group Innovations, Ottobrunn, Germany, where he is focused on design and applications of microwave filters in the field of microwave communication and sensor systems. His research interests include the design and theory of lossy microwave filters, millimeter-wave antennas, and microwave sensors.

Mr. Pflüger was the recipient of the VDI Förderpreis Award of the German Association of Engineers (VDI) in 2012.

Christian Waldschmidt (M'13–SM'13) received the Dipl.-Ing. (M.S.E.E.) and Dr.-Ing. (Ph.D.E.E.) degrees from the University Karlsruhe (TH), Karlsruhe, Germany, in 2001 and 2004, respectively.

From 2001 to 2004, he was a Research Assistant with the Institut für Höchstfrequenztechnik and Elektronik (IHE), TH. From 2004 to 2012, he was with the business units Corporate Research and Chassis Systems, Robert Bosch GmbH, Stuttgart, Germany, where he headed different research and development teams in high-frequency engineering, electromagnetic compatibility (EMC), and automotive radar. In 2013, he returned to academia and was appointed Director of the Institute of Microwave Engineering, University Ulm, Ulm, Germany, as a Full Professor. He has authored or coauthored over 80 scientific publications. He holds mover 20

patents. His research topics have included integrated radar sensors, radar system design, millimeter-wave technologies, antennas and antenna arrays, ultra-wideband (UWB), and EMC. His current research topics focus on radar and RF sensing, millimeter-wave and submillimeter-wave engineering, antennas and antenna arrays, multiple input–multiple output (MIMO), array signal processing, modulation techniques, and wave propagation.

Prof. Waldschmidt is a member of the ITG committee Microwave Engineering (VDE) and the IEEE MTT-27 Technical Committee (wireless enabled automotive and vehicular applications). He is a reviewer for multiple IEEE TRANSACTIONS and LETTERS.

Volker Ziegler (A'01–M'01–SM'09) received the Dipl.-Ing. degree in electrical engineering and Dr.-Ing. degree (with honors) from the University of Ulm, Ulm, Germany, in 1997 and 2001, respectively.

From 2002 to 2003, he was member of the Knowledge Exchange Group for Research and Technology, DaimlerChrysler AG, Stuttgart, Germany. During this trainee period, he was with the University of Michigan, Ann Arbor, MI, USA, and also with United Monolithic Semiconductors, Orsay, France. He then joined AIRBUS Group Innovations, Ottobrunn, Germany, where, in 2007, he became an AIRBUS Expert on Microwave Technologies and Systems. He is currently the Head of RF and Waveforms Team, responsible for the research performed in the field of key microwave technologies and waveforms for advanced radar and communication systems. He has authored or coauthored more than 70 papers. He served twice as an associate editor for the *International Journal of Microwave and Wireless Technologies*. He holds nine patents.

Dr. Ziegler is a member of the IEEE Microwave Theory and Techniques Society (IEEE MTT-S) Technical Coordinating Committee 21 on RF-MEMS and of the IEEE MTT-S Antennas and Propagation German Chapter Executive Board. He is also an industrial advisor for the ESA Component Technical Board on Microwaves.